Supplementary Information

2,3-diphenyl-5,6,7,8-tetrahydroquinoxaline based potential optical chemosensor for detection of Ni^{2+} ions: Anticancer activity and biosensor imaging

Srishti Dutta,[a] Dishen Kumar,[a] Abhilash Pandey,[a] Sounik Manna,[b] Sujata Maiti Choudhury,[b] Devanand Sahu,[a] Vanshika Sharma,[a] Niraj Kumari,[a] and Goutam Kumar Patra[a]*

[a]Department of Chemistry, Guru Ghasidas Vishwavidyalaya, Bilaspur (C.G)
[b]Biochemistry, Molecular Endocrinology and Reproductive Physiology Laboratory, Department of Human Physiology, Vidyasagar University (W.B.)

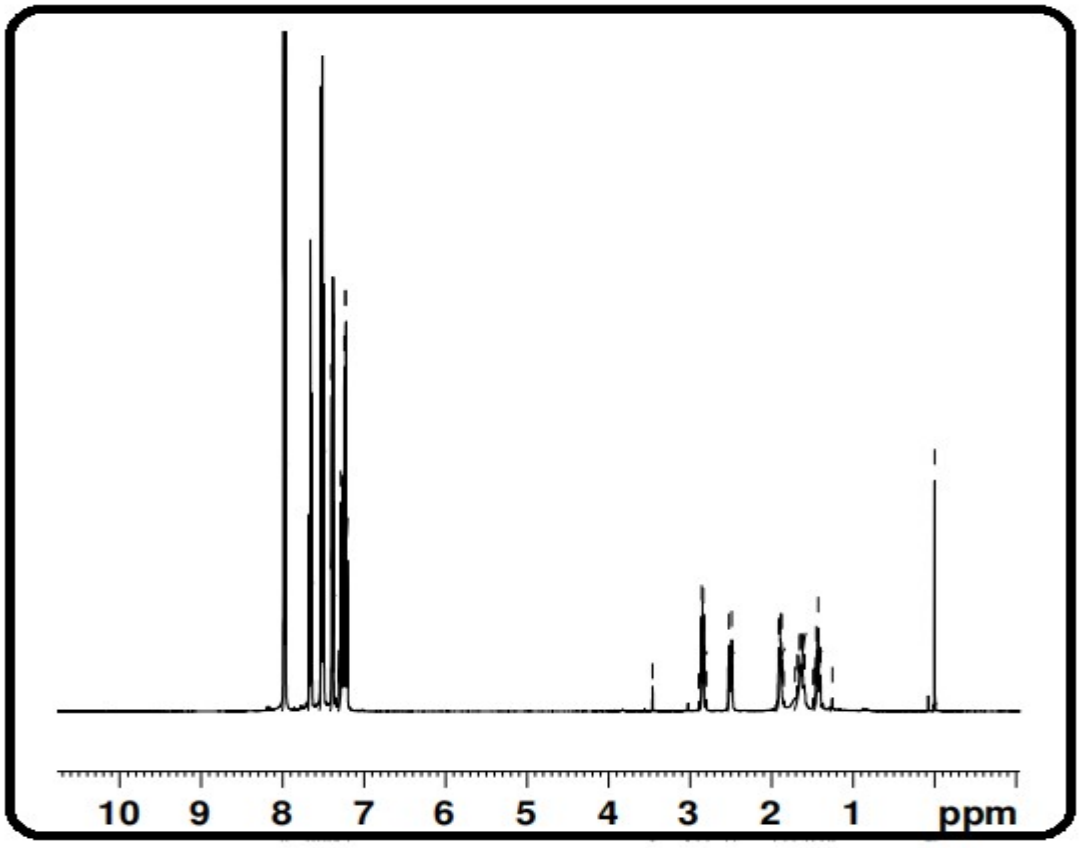

Fig. S1. ^{1}H-NMR spectra of **L** in $CDCl_3$

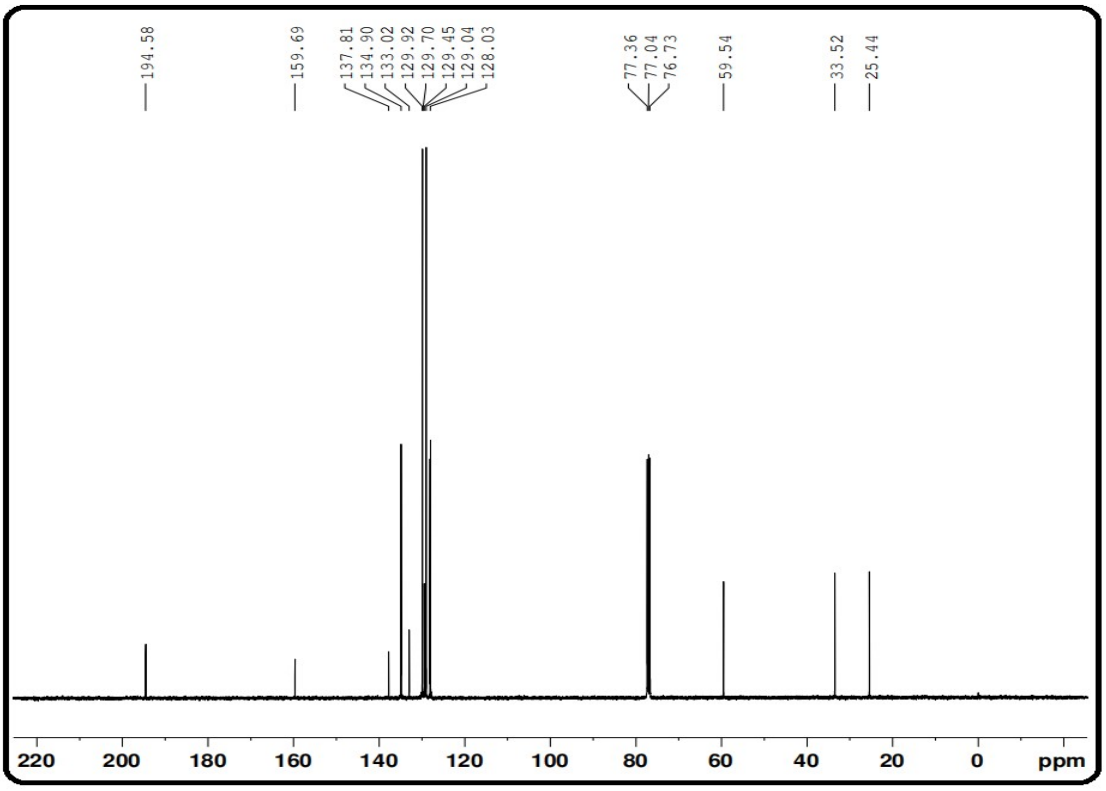

Fig. S2. ^{13}C-NMR spectra of **L** in $CDCl_3$

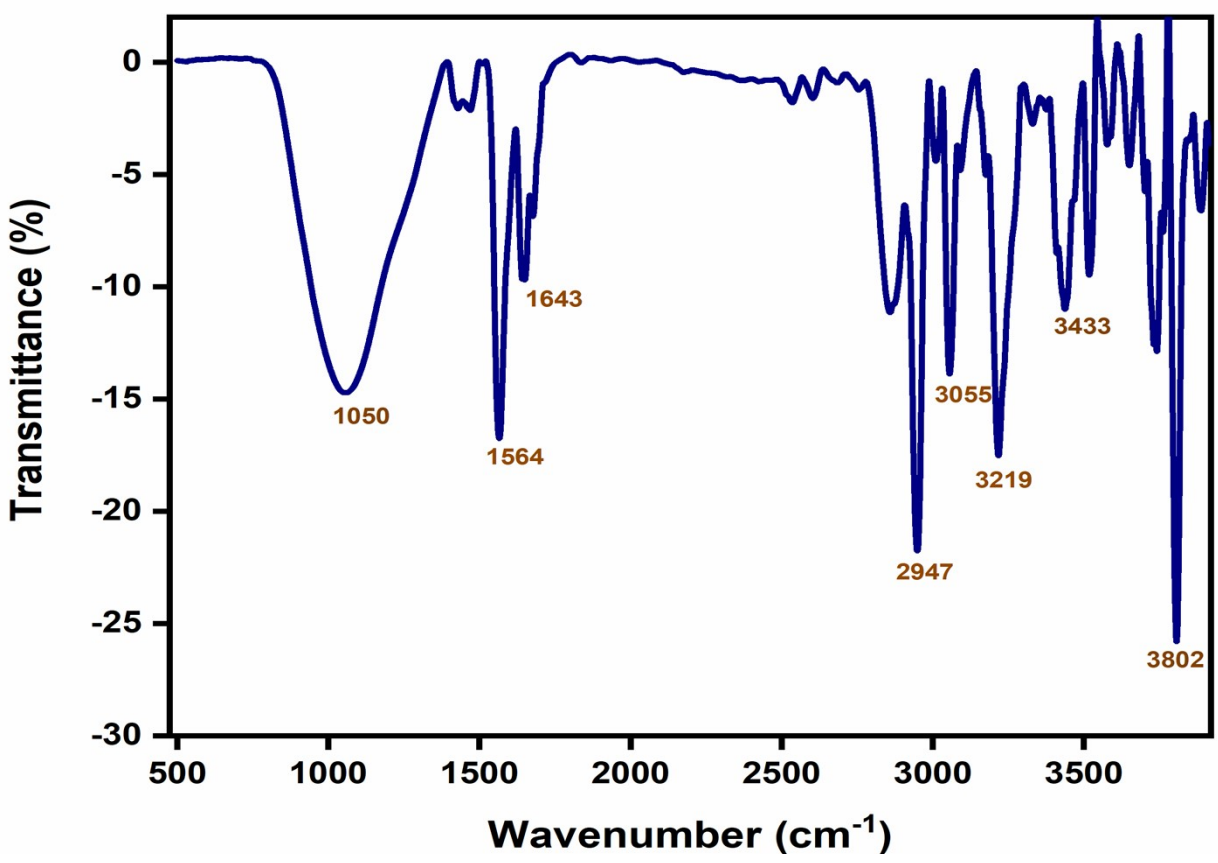

Fig. S3. FTIR spectra of **L**

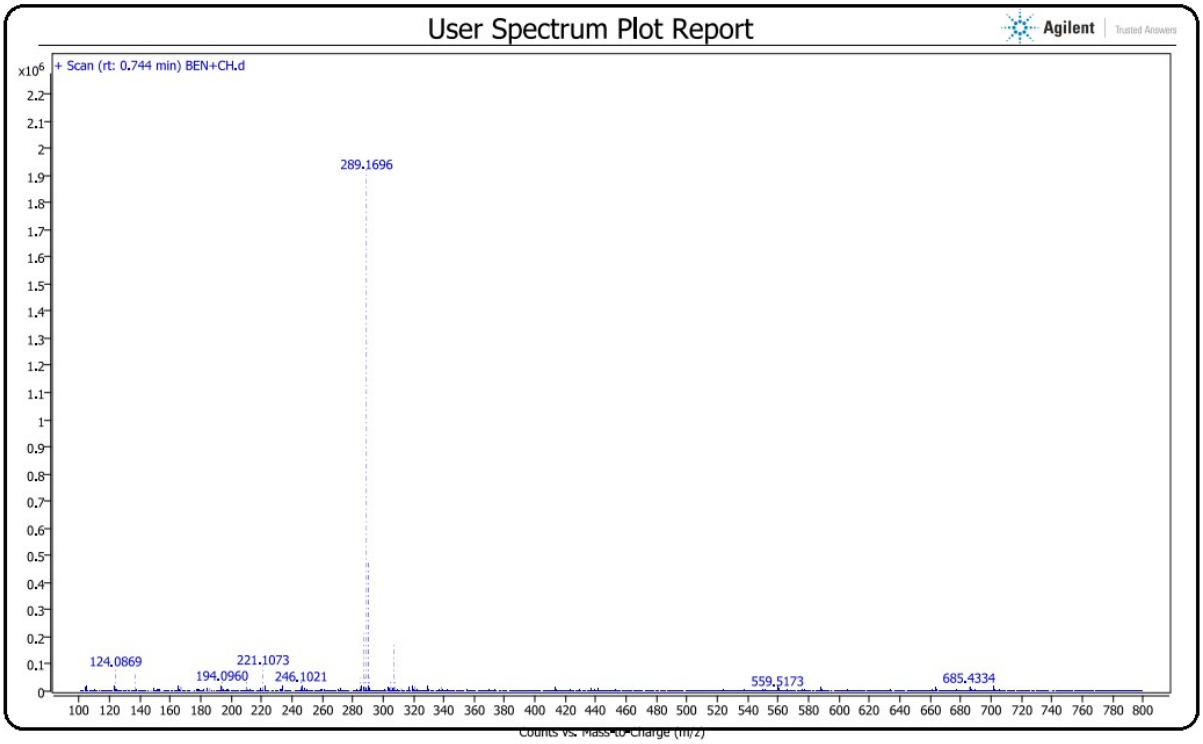

Fig. S4. Mass spectra of **L**

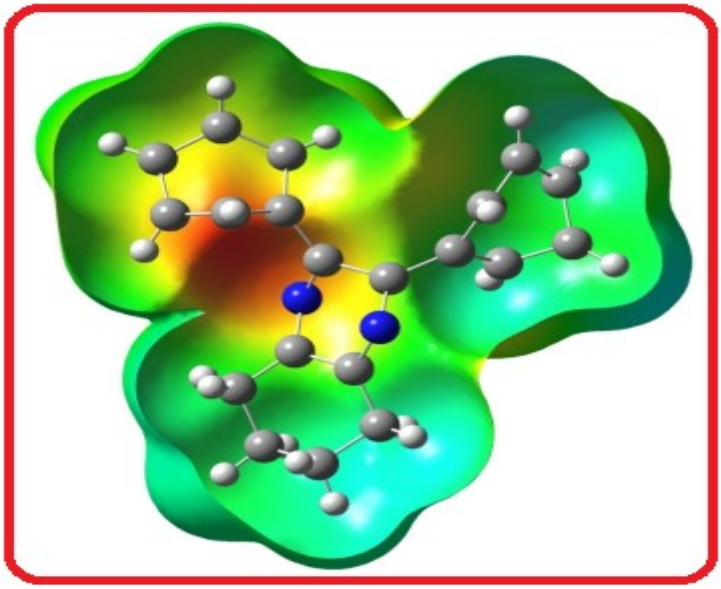

Fig. S5. Molecular electrostatic potential of **L**

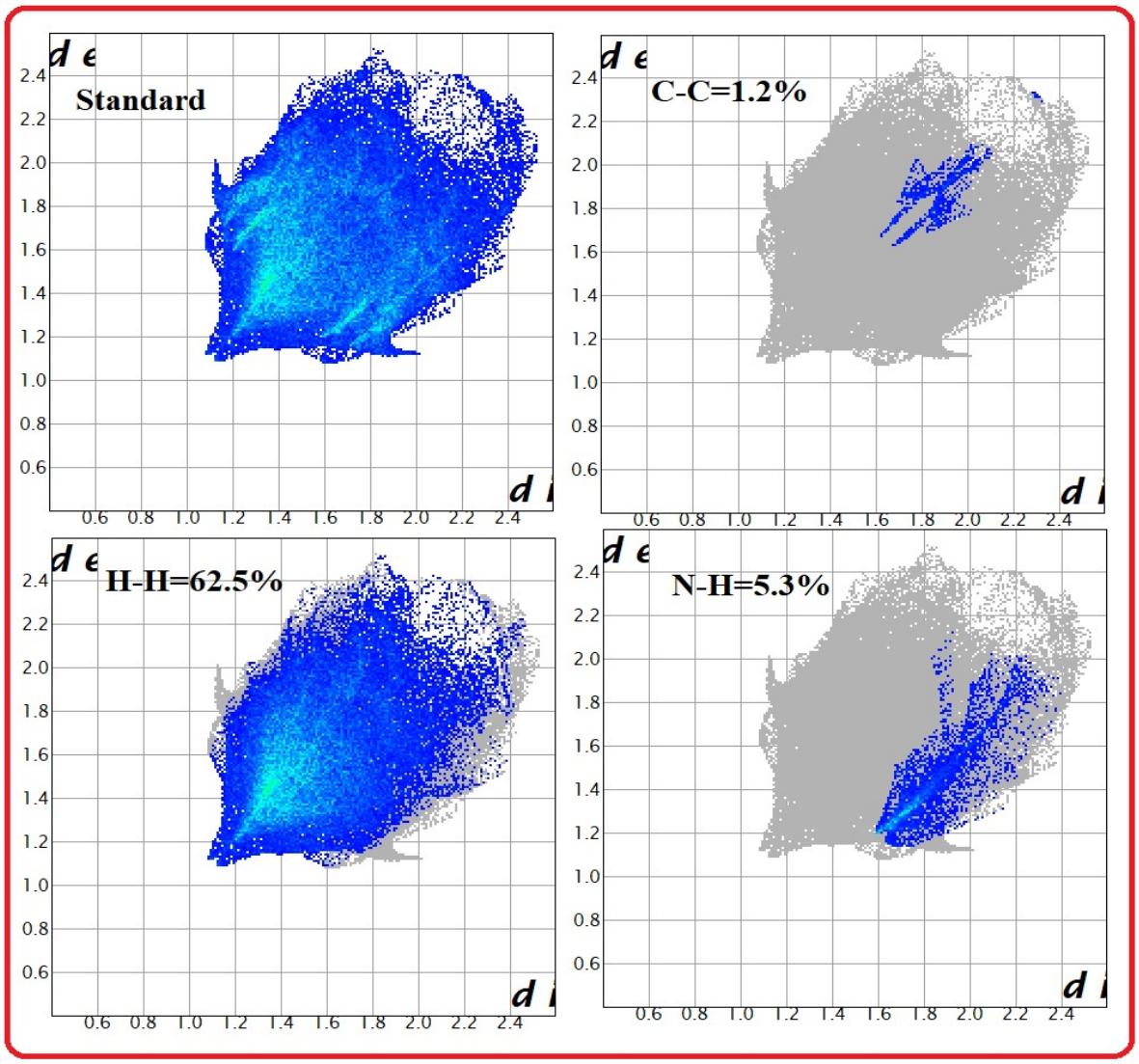

Fig. S6. 2D fingerprint plots of ligand **L**: (a) standard full and (b) resolved into C···C and (c) resolved into H···H (d) N···H contacts, showing the percentages of contacts contributing to the total Hirshfeld surface area of the molecule.

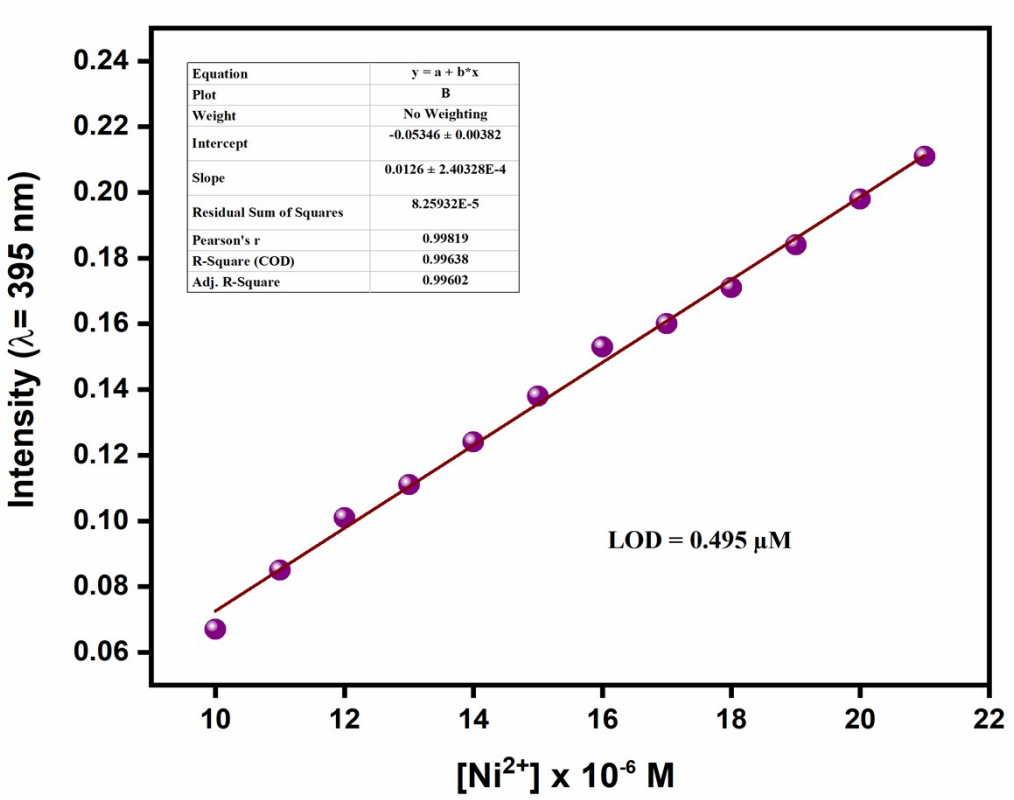

Fig. S7. Detection limit for Ni^{2+} from absorption titration spectra in CH_3OH-H_2O (1:1).

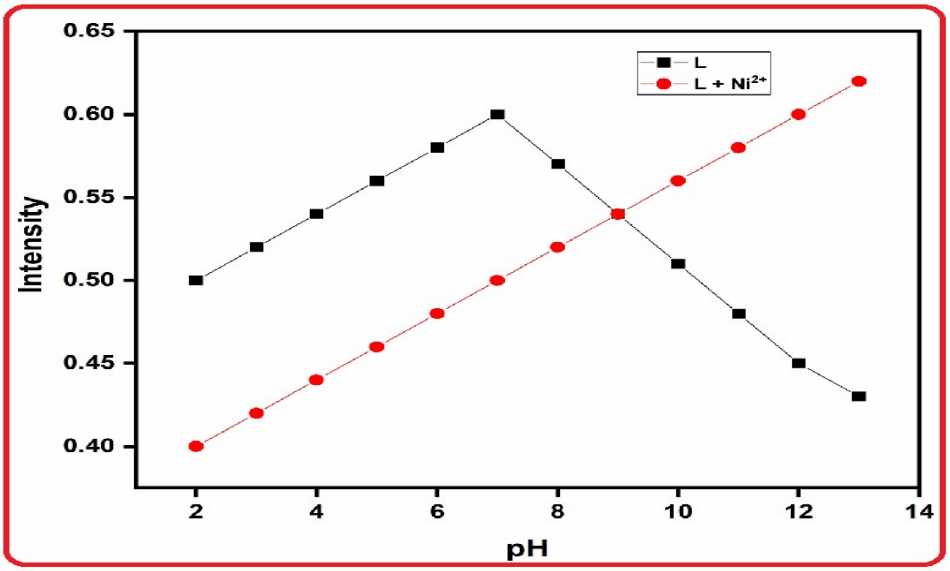

Fig. S8. Effect of pH (from range 2-13) on **L** in absorbance spectroscopy

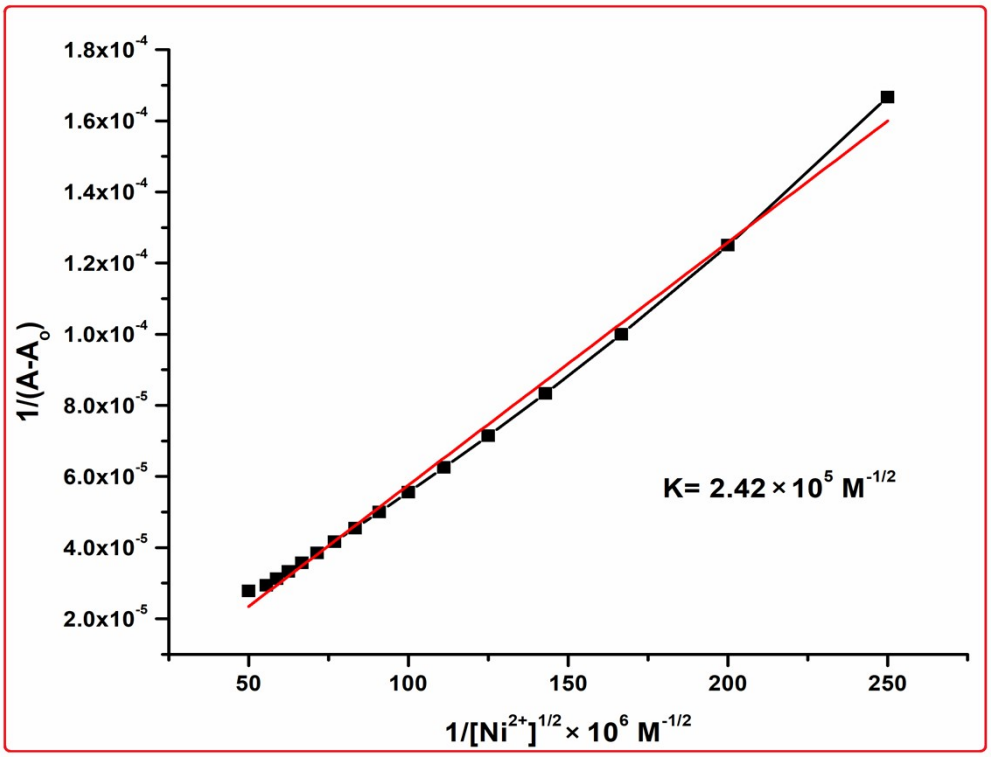

Fig. S9. Binding constant of **L**-Ni^{2+} complex.

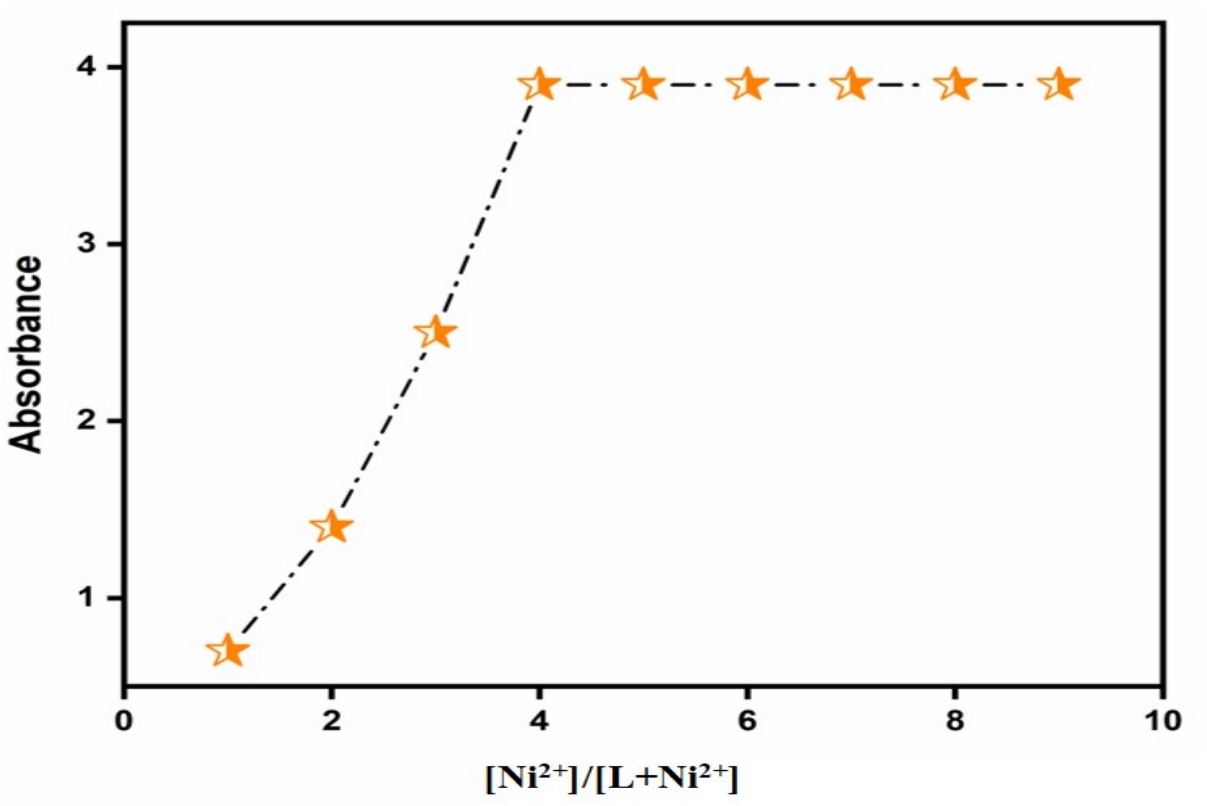

Fig. S10. Job's plot measurements of **L** by UV-Vis measurements.

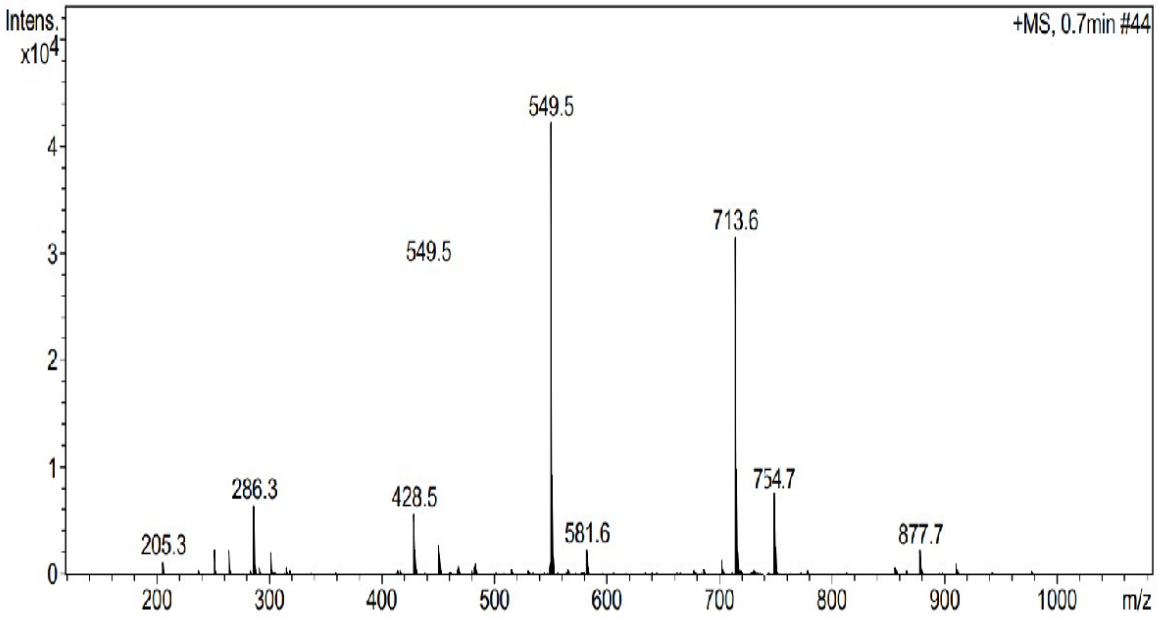

Fig. S11. ESI-MS spectra of **L**-Ni^{2+} complex.

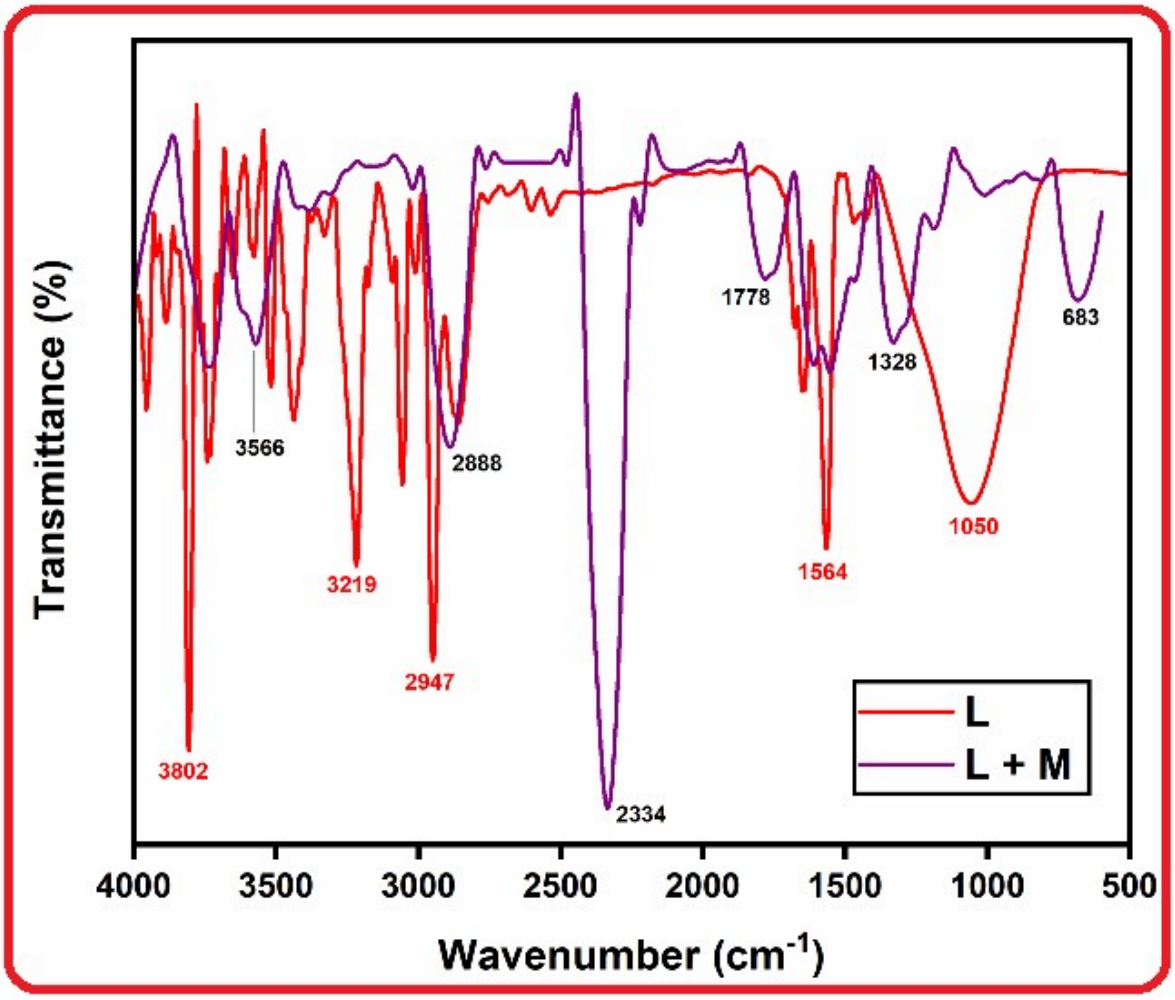

Fig. S12. Stacked plot of FTIR spectra of **L** and **L**+Ni^{2+} adduct

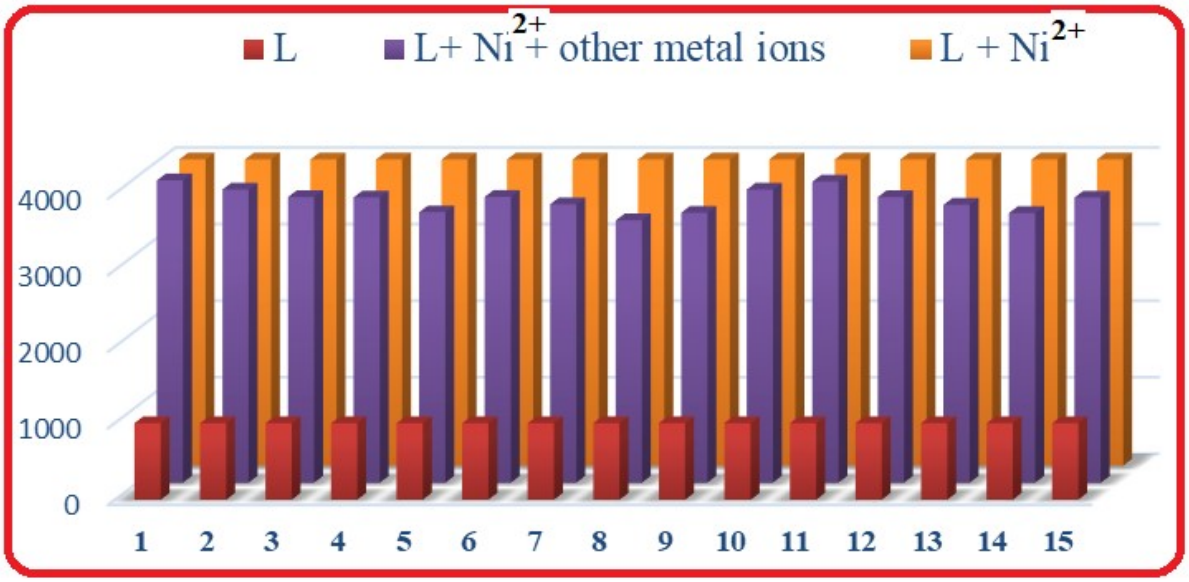

Fig. S13. Fluorescence interference study of **L**.